# Variation of the sticking of methanol on low-temperature surfaces as a possible obstacle to freeze out in dark clouds

K a K Gadallah, A. Sow, Emanuele Congiu, S. Baouche, F. Dulieu

MNRAS **000**, 1–12 (2020) Preprint 23 March 2020 https://doi.org/10.1093/mnras/staa862

# Variation of the sticking of methanol on low temperature surfaces as a possible obstacle to freeze out in dark clouds

K. A. K. Gadallah,[1,2]★ A. Sow,[1] E. Congiu,[1] S. Baouche,[1] F. Dulieu[1]†
[1]*CY Cergy Paris Université, Sorbonne Université, Observatoire de Paris, PSL University, CNRS, LERMA, F-95000 Cergy, France*
[2]*Astronomy&Meteorology Dept., Faculty of Science, AL-Azhar University, Nasr city, 11884, Cairo, Egypt*

Accepted XXX. Received YYY; in original form ZZZ

**ABSTRACT**
Sticking of gas phase methanol on different cold surfaces – gold, $^{13}CO$, and Amorphous Solid water ice (ASW) – was studied as a function of surface temperature (7 - 40 K). In an ultrahigh-vacuum system, RAIRS and TPD methods were simultaneously used to measure methanol sticking efficiency. Methanol band strengths obtained by RAIRS vary greatly depending on the type of the surface. Nevertheless, both methods indicate that the sticking of methanol on different surfaces varies with surface temperature. The sticking efficiency decreases by 30% as the surface temperature goes from 7 to 16 K, then gradually increases until the temperature is 40 K, reaching approximately the initial value found at 7 K. The sticking of methanol differs slightly from one surface to another. At low temperature it has the lowest values on gold, intermediate values on water ice and the highest values are found on CO ice, although these differences are smaller than those observed with temperature variation. There exists probably a turning point during the structural organisation of methanol ice at 16 K, which makes the capture of methanol from the gas phase less efficient. We wonder if this observation could explain the surprising high abundance of gaseous methanol observed in dense interstellar cores, where it should accrete on grains. In this regard, a 30% reduction of the sticking is not sufficient in itself but transposed to astrophysical conditions dominated by cold gas (∼ 15 K), it could reduce the sticking efficiency by two orders of magnitude.

**Key words:** ISM: molecules – methods: laboratory: solid state – methods: laboratory: molecular

## 1 INTRODUCTION

Methanol is the prototypical interstellar complex organic molecule (Herbst & van Dishoeck 2009; Caselli & Ceccarelli 2012), and is considered as a proxy for many others molecules (Ceccarelli et al. 2017). It is often used as an ideal tool for determining the physical conditions (Kristensen et al. 2010). Moreover, It has been observed in many different environments such as in dark clouds (Friberg et al. 1988), stellar cores in molecular clouds (Bisschop et al. 2007; Punanova et al. 2018), proto-stellar envelopes,(Taquet et al. 2015), circumstellar regions (Charnley et al. 1995), protoplanetary disks (Walsh et al. 2016, 2018), young stellar objects (Bottinelli et al. 2010; Penteado et al. 2015), comets (Bockelee-Morvan et al. 1991), and extragalactic environments (Galametz et al. 2016). Often, in warm environments, ice mantles can release methanol to the gas-phase by means of thermal desorption. But in the coldest and darkest places such as pre-stellar cores, gas phase COMs are not expected to be as abundant as observations suggest (Bacmann et al. 2012; Jiménez-Serra et al. 2016, 2018; Punanova et al. 2018). The enigma of the presence of COMs in the gas phase at low temperature in the dense phases of the interstellar medium stems from the fact that that COMs and any other molecule (except $H_2$) should condense onto dust grains within a short timescale (Bergin & Tafalla 2007).

There are different possibilities to explain the unexpected high abundances of COMs. One of them is that there are different non-thermal mechanism at work desorbing the adsorbed species. One possible mechanism is the chemical desorption (Dulieu et al. 2013). Indeed, after a reaction on a cold surface, the excess of energy can induce the return in the gas phase of the products. Therefore, methanol can be released in the gas phase during its formation on dust grains, and this process can be specifically efficient in the case of CO hydrogenation (Minissale et al. 2016a). Vasyunin & Herbst (2013) have demonstrated that methanol gas-phase abun-

★ E-mail: k.gadallah@azhar.edu.eg
† E-mail: francois.dulieu@obspm.fr

dance in different astrophysical environments can be explained by the desorption of a few per cent of methanol formed on the grain surfaces. Using revised experimental values of Minissale et al. (2016b),Vasyunin et al. (2017) successfully reproduced the abundance and the position of COMs of the L1544 prestesellar core.

Another possibility of non-thermal desorption is the sputtering by cosmic rays of solid methanol, as measured by Dartois et al. (2019) which releases intact molecules into the gas phase, contrarily to UV photons which easily photolyses large molecules (e.g., Cruz-Diaz et al. 2016; Bertin et al. 2016), and therefore mostly returns fragments in the gas phase. Similarly, electron irradiation of water ice (Gadallah et al. 2017; Marchione & McCoustra 2017) releases simple molecules such as $H_2$, HD and $D_2$ more efficiently than larger ones. Latter authors have shown that $H_2$ formation is more significant for organic-based ices, such as methanol ice, than in water ice. This might indicate that processes driven via electronic excited states produced by dipole scattering of the CR in solid methanol do not produce significant molecular methanol.

In addition to the formation of small molecules (e. g. formaldehyde, methane, carbon monoxide, carbon dioxide, and water), the VUV photo-processing of methanol ice (Paardekooper et al. 2016) has also produced COMs such as methyl formate, ethylene glycol, dimethyl ether. This process reveals a reverse relationship between the rest of methanol and other outcomes with increasing the VUV fluence. Similar VUV photolysis with much longer irradiation of methanol ice (Abou Mrad et al. 2016) has produced small molecules and COMs with a variety of carbon chain, where abundances of these COMs decrease with increasing their carbon chain.

The other possibility to solve the enigma of the presence of certain molecules in the gas phase in dark and cold media is that there exist selective mechanisms to inhibit the accretion of some molecules. Nguyen et al. (2018) have studied the case of surface CO molecules that change the adsorption properties of $N_2$, but it cannot apply for larger molecules. A difference of sticking probability for some specific molecules or under specific conditions would also greatly affect the gas phase composition and would explain how some molecules can be maintained in the gas phase.

This is the starting point of the present study. However, the sticking of molecules like $H_2O$, $CH_4$, $N_2$ and CO has already been studied (Kimmel et al. 2001; Acharyya et al. 2007; Bisschop et al. 2006), and it has always been claimed to be "close to unity", and as such rounded to one in models. There is an exception in the case of $H_2$ and $D_2$ (Matar et al. 2010; Chaabouni et al. 2012) since it has been measured to be as low as 25%. This is due to the fact that a molecule has to lose some initial kinetic energy when impinging the surface, and if the energy loss is not efficient enough, the impactor just bounces back. Therefore, the sticking probability is dominated by the ability of the surface to evacuate the excess energy of the impactor. In the case of $H_2$ the mass match is very poor and this is why the sticking coefficient is rapidly decreasing with the temperature of the gas (the impactor). But the sticking coefficient, extrapolated at 0 K is not 100%. This is not obvious because one could consider that the probability of capture of the impactor should be unity since there is no energy to dissipate and/or since the interaction time is infinite, and that the energetic balance is favourable to adsorption. But this is only true if there is no entrance barrier, in this case some kinetic energy of the impactor is required to pass the saddle point. In other terms, sometimes the substrate has to be slightly geometrically reorganised and this requires some energy, which may be provided by the kinetic energy of the impactor.

Sometimes, the molecules can react with the surface as it is the case of methanol on a platinum surface (Diekhöner et al. 1998). On platinum, also the probability of its decomposition decreases as a function of both the surface temperature (400-1000 K) and the incidence energy (<0.5 eV) of methanol.However, metallic surfaces are of low interest for astrophysics. To date, there is no complete study of the sticking of methanol at cold temperatures. On the contrary there are many studies about its desorption (Sandford & Allamandola 1993; Collings et al. 2004; Wolff et al. 2007; Bahr et al. 2008; Green et al. 2009; Smith et al. 2014; Doronin et al. 2015; Luna et al. 2018). In these experiments we can learn that the methanol ice structuring can be complex.

In this paper, we study the sticking of methanol on cold surfaces as a function of surface temperature ($T_s$) in the range 7 – 40 K. The surfaces are made of gold, $^{13}CO$, and pours amorphous solid water (ASW). We measure the total molecules adsorbed by using both temperature-programmed desorption (TPD) and, in situ, using the Reflection Absorption Infrared Spectroscopy (RAIRS). The experimental set-up will be described in Sec. 2, while the results will be shown and discussed in detail in Sec. 3. The astrophysical implications and conclusions will be given in Sec. 4 and 5, respectively.

## 2 EXPERIMENTAL SET-UP

### 2.1 Apparatus

To conduct our experiments, we used the new apparatus called VENUS (VErs de NoUvelles Synthèses), an Ultra-High Vacuum (UHV) system based in the LERMA laboratory at the University of Cergy-Pontoise (Congiu et al. 2020). VENUS consists of three stainless steel chambers. The first two (chambers 1 and 2) have a pressure of $10^{-8}$ and $10^{-9}$ mbar, respectively, and are used as differential pumping stages for the beamlines. The third one is the main chamber in which the pressure never exceed $2{\times}10^{-10}$ mbar. Inside the main chamber, a sample holder is mounted onto the cold head of a closed-cycle He cryostat. The sample holder is made of a circular copper mirror coated with gold. Its temperature can be varied in the range 7 – 350 K and it is computer-controlled by a variable resistive heater. The main chamber is also equipped with a quadrupole mass spectrometer (QMS) that can translate vertically and be placed at 5 mm in front of the sample holder. Simultaneously, the beam of a Fourier Transform InfraRed Spectrometer (FTIRS) falls on the sample surface with a grazing angle of 85°. In addition to the background line used for direct water vapour dosing inside the main chamber, the apparatus also includes several independent beam lines (up to 5 beam lines) passing through the expansion chambers 1 and 2, and finally to the main chamber via five 2-mm diaphragms aligned with the surface sample. One of beam lines was used for injecting an effusive molecular beam of $CH_3OH$.

### 2.2 Experiments

Under the UHV conditions of VENUS, many experiments were performed to form very thin layers of methanol on three different cold surfaces (gold, $^{13}CO$, and porous ASW) at very low surface temperatures ($T_s$). The gold surface consists simply of the polycrystalline gold layer coating the sample holder. $^{13}CO$ and ASW ice substrates are obtained by depositions onto the gold surface previously to methanol dosing. As for deposition techniques, both $^{13}CO$ and methanol were injected using two different beam lines, while water was introduced in the main chamber using the background line. Prior to each experimental run, both methanol and water were purified by doing multiple freeze-pump-thaw cycles.

For all gas injections, whether via the beam lines or the background line, the thickness of the deposited species was calibrated relative to a given pressure and injection duration. For this calibration, TPD techniques were used to determine one monolayer (1 ML) using the method of multilayer peak appearance (Noble et al. 2012; Nguyen et al. 2018). The $^{13}CO$ layer was deposited using a gas flow of 0.3 sccm (standard cubic centimeter per minute) giving a pressure of $2 \times 10^{-4}$ mbar within the beam line before entering into chamber 1. Under these physical conditions, a 1-ML layer of $^{13}CO$ is formed every 6.5 minutes. To deposit an ASW ice layer via the background line, a leak valve is used to inject water vapour into the main chamber. 1 ML of ASW ice is formed by injecting $10^{-8}$ mbar of water vapour per 2 minutes. The methanol is dosed via one of the beam lines and 1 ML is formed every 8 minutes by using a pressure of $\sim 2 \times 10^{-4}$ mbar of methanol gas in the injection chamber. We first have grown films of methanol on the golden mirror at 14 different values of $T_s$ ranging from 7 to 40 K. During each experiment, FTIRS measurements were carried out every two minutes while the TPD measurement was done at the end of the deposition phase. These experiments were repeated two more times to form a film of methanol on predeposited samples of $^{13}CO$ and ASW ices. The $T_s$ values were chosen taking into account a small variation (1 K) at lower temperatures, that is $T_s$=7, 8, 9 K and then with a larger variation (5 K) at higher values. When the $^{13}CO$ layer is deposited as an underlayer for methanol films, both species are deposited at the same $T_s$. On the other hand, the ASW ice substrate was deposited at 42 K, so as to ensure that the morphology of the ice remained unchanged during all the experiments carried out at all $T_s$ values. Of course, the ASW ice structure evolves during the TPD above 42 K, but not during the deposition phase of methanol, which is key for studying sticking properties.

The TPD mass spectra are primarily used to measure the desorption of methanol molecules from the cold surfaces. The peak integrated area ($A_{TPD}$) as a function of the surface temperature is used to measure the methanol sticking. All TPD experiments were performed with a heating ramp of $\beta = 0.2$ K s$^{-1}$, and FTIRS spectra were baseline corrected.

## 3 RESULTS AND DISCUSSION

TPD experiments provided many mass spectra of methanol (m/z=32) as QMS signals (cps) or desorption rate (molecules cm$^{-2}$ s$^{-1}$). Of relevance to the sticking of methanol, the results of TPD and RAIRS spectra were quantitatively analysed. In the following subsections, we show in detail the sticking profiles derived from $CH_3OH$ desorption under different temperature initial conditions and from different surfaces.

### 3.1 Methanol beam flux

For all experiments, methanol gas was injected at the same pressure ($\sim 2 \times 10^{-4}$ mbar) that was used for calibrating the methanol layer thickness. Keeping this pressure in the injection chamber, the beam flux ($\Phi$) was measured with the QMS facing the beam and placed in front of the surface. QMS signals in counts per seconds (cps) were measured before and after each experiment and vary slowly from one experiment to the next. We attribute the methanol flux instability to fluctuations of ambient temperature of the room.

For all $T_s$, the values of $\Phi$ are shown in Fig. 1 as red open circles on the gold surface (left panel), on the $^{13}CO$ substrate (central panel) and on the ASW substrate (right panel). Also the integrated areas of $CH_3OH$ TPD peaks ($A_{TPD}$) are presented in this figure (black open squares). TPD profiles will be described in the following subsection according to thickness and $T_s$. The horizontal dashed-line on Fig. 1 represents a reference of 700 cps corresponding to the normalisation of $\Phi$.

First, we note that the relative variations of $\Phi$ are much smaller than the relative variations of $A_{TPD}$. The measurements are not directly comparable, since the TPDs measure a signal area over the entire desorption time, while the flux is a simple average per unit time. That being said, we notice that the $A_{TPD}$follow approximately the fluctuations of the $\Phi$: low fluxes corresponding to low desorption areas, and vice versa. There are, however, some data against this general trend, for example on the gold surface (left panel) the highest $A_{TPD}$ is at 40 K (around 4600 cps K), whereas for a similar flux the point at 14 K is around 3500 cps K. Moreover, if we repeat the experiment at the same temperature, but using a different flux, the ratio $A_{TPD}/\Phi$ is remarkably constant. Thus, if we consider that the ratio of the incoming molecules (measured by the flux) and of the desorbing molecules (measured by the TPD area) represents the sticking coefficient S, we can calculate S($T_s$) after normalising the incoming flux $\Phi$ to the average value of 700 cps, and $A_{TPD}$to its highest value at $T_s$ = 40 K. By doing so, we assume a sticking coefficient of unity at 40 K. The variation of S($T_s$) will be analysed later.

Fig. 2 shows the ratio of the non-normalized $A_{TPD}$over S($T_s$) as a function of $\Phi$. As expected, it shows a linear trend, and we would like to point out that the experimental deviation from this straight line (determined by repeated experiments) is less than 2%. Moreover, this ratio runs linearly to zero indicating that our measurements of both $\Phi$ and $A_{TPD}$are exempt from noise, and that the normalisation of the flux allows us to extract the sticking coefficients as a function of temperature, in a very larger extent than our experimental uncertainty.

### 3.2 Methanol TPD profiles

QMS measurements have two essential properties for this study: they are stable and have a very good detection sen-

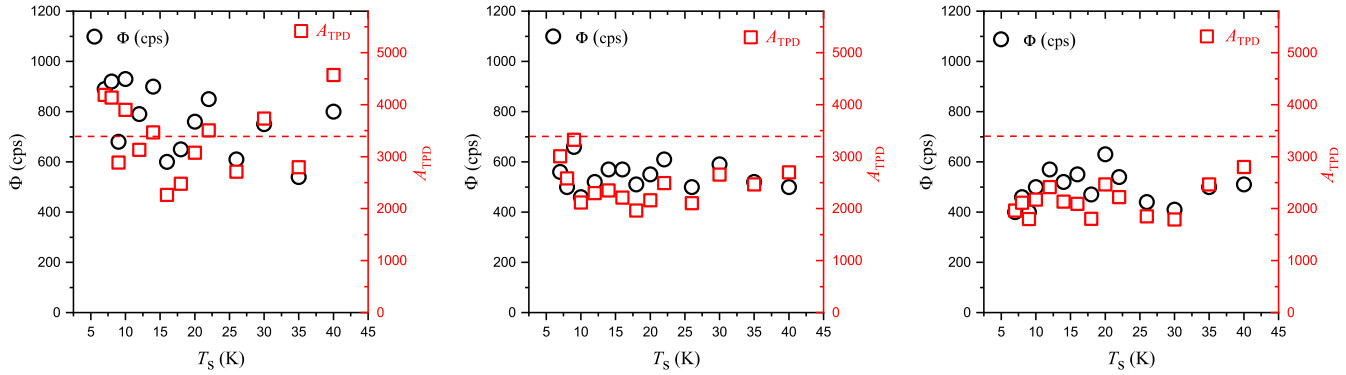


**Figure 1.** The beam flux (red circles) and integrated TPD area ($A_{TPD}$) of methanol (black squares) on the right and left vertical axes, respectively, versus the surface temperature $T_s$, on gold (left panel), $^{13}CO$ (middle panel) and ASW ice (right panel).

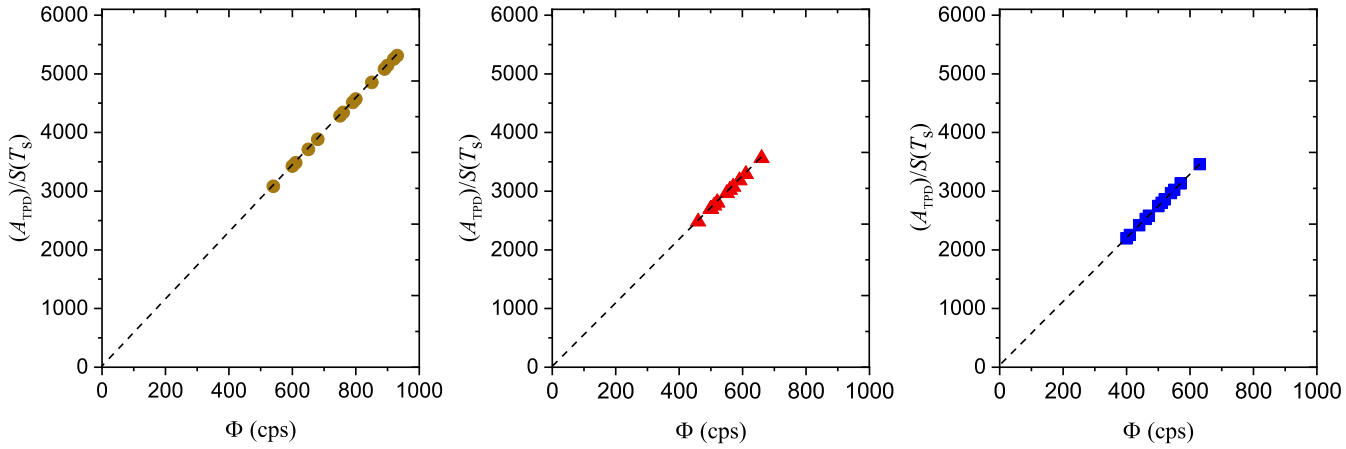


**Figure 2.** Ratio of $A_{TPD}$ to the sticking S($T_s$), as a function of beam flux of methanol on the substrates of gold (left panel), $^{13}CO$ (middle panel), and ASW ice (right panel).

sitivity. The drawback of this method is that it cannot give direct information on the solid phase, but only measures what is being deposited (Φ) and what is desorbing (TPD). Fig. 3 shows some TPD profiles of methanol at coverages of 0.5, 0.75, 1, 2, and 3 ML on the gold substrate held at $T_s$=10 K. They present a maximum of desorption around 135-138 K in agreement with published results, given our temperature ramp, coverages and substrate. The curves for 1, 2 and 3 ML (magenta, red and green curves, respectively) present a common leading edge characteristic of the multilayer regime. The inset of the figure shows $A_{TPD}$(normalised by the flux) as a function of coverage. It shows a proportional increase of the desorption rate with the dose. The deviation of the experimental points from the linear fit is very small and indicates a constant sticking, independent from the coverage.

At a specific thickness of 1 ML of methanol, TPD profiles were carried out at different deposition temperatures ($T_s$ between 7 and 40 K) on the three cold substrates. In Fig. 4, we show some examples of these profiles (taken at $T_s$= 7, 16, 40 K) from gold (top panel), $^{13}CO$ (middle panel) and ASW (bottom panel). The overview on the top and middle panels corresponding to gold and $^{13}CO$ surfaces, respectively, shows that methanol has a similar desorption peak at $(T_d)_{max}$ ~ 137 K from both substrates. This peak position is marked by the orange dotted line in Fig. 4. In addition to this feature, another additional peak of methanol desorption appears having $(T_d)_{max}$ ~ 152 K on ASW surface as marked by a dashed violet line. This second peak is the signature of co-desorption of methanol and water. This was expected since the morphology of water ice grown at 42 K is porous, and some trapping and mixing between $CH_3OH$ and $H_2O$ is very likely to occur during the linear heating of the ices. Moreover, we can see that the balance between the peak at $(T_d)_{max}$ =137 K and the peak at 152 K changes with deposition temperature. At the lowest deposition temperatures there is less co-desorption of water and methanol, that is less mixing, while at $T_s$=40 K we observe the largest co-desorption effect. This indicates that the spreading of methanol on water ice is different depending on the surface temperature at the time of deposition. At the lowest $T_s$, methanol molecules find adsorption sites on the outer surface of the water film, while they can rearrange more at higher temperatures and are in stronger interaction with the

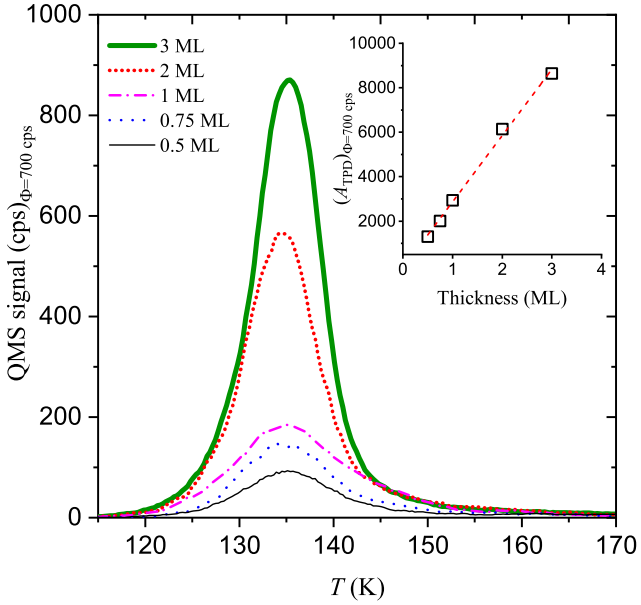


**Figure 3.** The TPD mass spectra of various doses of methanol (at the normalised flux Φ=700 cps) from gold hold at $T_s$=10 K. Inset: methanol $A_{TPD}$ normalised by the flux, as a function of deposition thickness.

porous icy substrate. This is a known phenomenon that has been described during the study of the variation in water morphology with deposition temperature by B. Kay's group Kimmel et al. (2001).

From all three different surfaces, however, it is clear that the desorption of 1 ML of methanol deposited at $T_s$=16 K shows the lowest peak area, whilst in the experiments where methanol is deposited at 7 and 40 K the desorption peaks have the largest and similar areas. This leads us to conclude that at 16 K it is very likely that fewer molecules have stuck, since fewer molecules have eventually desorbed. Therefore, the sticking of molecules would depend on the surface temperature at the time of deposition, even if such temperature is much lower than the sublimation temperature.

### 3.3 RAIRS measurements of methanol layers

Even if RAIRS has lower sensitivity than that of the QMS, infrared spectra have provide the great additional advantage of measuring the quantity of molecules adsorbed on the surface. RAIRS spectra were acquired under UHV conditions as mentioned in Sec. 2. Fig. 5 shows the RAIRS spectra obtained during the growth of the methanol film on the gold surface at $T_s$=10 K. They are characterized by the growing methanol featrures; the O-H stretching vibrational mode around 3235 cm$^{-1}$, the C-H asymmetric stretching plateau around 2940 cm$^{-1}$, the C-H symmetric stretching mode at 2830 cm$^{-1}$, the broad C-H bending modes around 1460 cm$^{-1}$ and the C-O stretching band at 1045±5 cm$^{-1}$. The plateau from 1080 to 1200 cm$^{-1}$ is rather noisy, as can already be seen in the reference spectra. The C-O stretching feature was the band used to evaluate the thickness of the methanol layer. We used the Lorentzian fitting method to calculate its integrated area, $A_{IR}$(1045±5 cm$^{-1}$). A RAIR spectrum

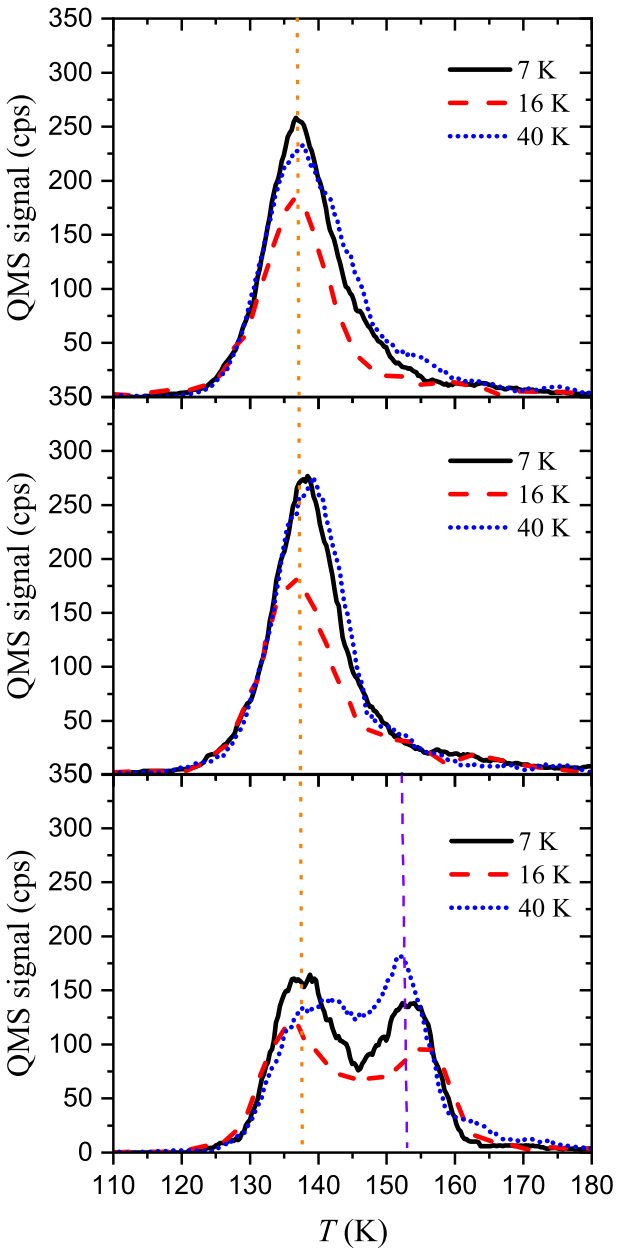


**Figure 4.** Some of methanol TPD mass spectra normalized to depositions at Φ=700 cps, deposited at different values of $T_s$ on surfaces of gold (top panel), $^{13}$CO (middle panel) and ASW ice (bottom panel). The orange dotted line refers to methanol peak desorption at approximately $(T_d)_{max}$ =137 K and the violet dashed line refers to desorption at approximately $(T_d)_{max}$ =152 K appearing only on ASW surface.

was acquired every two minutes during the deposition. We remind that 1 ML corresponds to 8 minutes of deposition time under our experimental conditions. The top panel of Fig. 6 shows the fitted $A_{IR}$(1045±5 cm$^{-1}$, of a continuous deposition of methanol on gold surface held at 10 K. We have calculated the slope ($\alpha$) as a function of the layer thickness as shown in Fig. 6 (bottom panel). The error bars are calculated as standard deviations of the linear fit. The first point

has no uncertainty since a unique line connect two points, and so give a unique slope. We see that $\alpha$ decreases with the methanol thickness until nearly 1 ML, then it becomes stable with increasing thickness. This reduction is probably due only to the decrease in the error bar as $\alpha$ converges towards its average value. Therefore, we conclude that with a thickness of 1 ML we can obtain a good estimate of $\alpha$, which remains constant beyond this value of the coverage. As we want to study the effect of the substrates, this is also the appropriate thickness that should enhance the differences between each of them.

We systematically measured the RAIRS spectra during the deposition of ~ 1 ML (8 minutes) of methanol and analyzed the growth of the peak area at 1045 $cm^{-1}$, for the three types of surfaces and at various deposition temperatures from $T_s$=7 to 40 K. Some of these spectra (at $T_s$=7, 10, 16, 20, 30 and 40 K) are shown in Fig. 7 on the substrates of gold (top panel), $^{13}CO$ (middle panel), and ASW ice (bottom panel). The $^{13}CO$ underlayer can be seen by its absorption peak at 2094 $cm^{-1}$, whereas the water substrate spectral signature is not visible because we have reset the reference spectrum prior to injecting the methanol, due to the necessary delay between water ice deposition and return to the best UHV conditions. The calculation of the coefficients $\alpha$ versus $T_s$ for the different substrates makes it possible to compare the different growth behaviour of methanol. The trend profiles of $\alpha$ as a function of $T_s$are displayed in the top panel of Fig. 8. We can see that their behaviours are similar and vary with increasing $T_s$ for the three surfaces. These profiles decrease with increasing $T_s$ until 16 K on all substrates. Above this temperature, $\alpha$ gradually increases again with $T_s$. Obviously, the $\alpha$ profiles show a parallel trend for all surfaces, namely they decrease at lower temperatures between 7 and 16 K then they invert the trend and increase from 16 K to 40 K. An exception appears marginally on the profile $\alpha$ on $^{13}CO$ to $T_s > 25$ K (empty triangles, Fig. 8) where a slight negative deviation is observed. This is probably due to the fact that above 25 K the $^{13}CO$ sublayer begins to desorb. Therefore, for temperatures between 25 and 40 K, there is only a fraction of a monolayer of CO on the surface, which is thus made up of a growing part of gold. In fact, we can see that $\alpha$ values on $^{13}CO$ tend towards those measured on bare gold.

The three trends are parallel, and there is a maximum absolute difference of a factor of two. We can then ask ourselves if it is because there are twice as many molecules or if it is because of the band strengths – which we know are very sensitive to the molecular environment (Palumbo 2006; Öberg et al. 2007; Fulvio et al. 2009; Palumbo et al. 2010) – are twice as strong, especially on a water substrate. The QMS measurements that will be discussed below suggest that the number of molecules is identical, so we conclude here that methanol band strengths differ by a factor of two between a gold surface and an ASW ice. We may also ask if our method of analysis (fit of the 1045 $cm^{-1}$ band) is to be questioned. Indeed it can be sensitive to the deformations of the band, and not only to its change in intensity. We point out here that a direct integration, given the weakness of our signals, gave noisier results. But in any case, we used the same method, and the only difference lies in the type of substrate. This reminds us of how much the infrared band strengths of the same molecule can vary from one system/environment to another. Finally, we note here that unlike many other infrared measurements done in similar studies, we did not use thick ices, whose bulk averages environmental effects.

In order to compare in detail the effect of the substrate, we have normalized $\alpha$ profiles relative to the value at 40 K ($\alpha_{max}$). The bottom panel of Fig. 8 shows a remarkable difference as $T_s$ decreases. At the lowest $T_s$, the $^{13}CO$ layer shows the highest sticking probability while the gold surface shows the lowest one. However, the variation with the temperature is more important than the effect of the substrate. As a result of the trend profiles of $\alpha$, the sticking of methanol shows approximately a 30% reduction around 16 K compared to the values obtained at 7 and 40 K.

### 3.4 Sticking versus surface temperature

The RAIRS data clearly show that the $\alpha$ coefficients vary with $T_s$. On the other hand, because the band strength may vary according to the environment, and since the morphology/topology of the methanol film is different according to the deposition temperature, as we have seen previously by examining the fraction of the co-desorption with water, we do not know if it is a variation of the sticking or only a variation in the band strength. Unlike RAIRS spectra, QMS data are not affected by variations of detection efficiency.

The profiles of $A_{TPD}$ are shown in the the top panel of Fig. 9 as a function of $T_s$ (7 – 40 K). They have been corrected to take into account the variations of the methanol flux. The areas of the TPD peaks of methanol show a variation with $T_s$. The behaviour of this variation is in agreement with what is observed in the trend of $\alpha$ profiles derived from RAIRS spectra. Moreover, the spread of the values for the different substrate is low compared to the variation with $T_s$.

The bottom panel of Fig. 9 shows quantitatively the sticking of methanol molecules as a function of $T_s$, assuming that the sticking is one at 40 K on all substrates. Like with RAIRS data, we also observe a reduction of methanol molecules of around 30% at 16 K. Among all surfaces, methanol sticking profiles have slight differences in the sticking at lower surface temperatures: the lowest sticking is found on gold and the highest one is found on the $^{13}CO$ surface. We now compare the two bottom panels of Fig. 8 and Fig. 9, and find that they are very similar. The trend presented in Fig. 8 is consistent with that in Fig. 9, which comes from the TPD. This perhaps can be seen as further evidence that the trend is real. There are slight differences in the temperature range 12 to 14 K. The initial decrease with $T_s$ appears to be slightly steeper with RAIRS data, maybe indicating that the bands strengths may have slightly varied there, but this is too close to our experimental uncertainties to be conclusive.

The trend in methanol sticking profiles raises an open question about the origin of the reduction in methanol sticking around $T_s$=16 K. To explain this point simply, it seems that there are two antagonistic mechanisms concerning the methanol sticking. One mechanism increases the sticking efficiency with surface temperature and the other decreases it, and their effect is reversed around 16 K.

The origin of these two mechanisms might lie in the bonding of methanol on cold surfaces. Methanol is composed of a methyl -$CH_3$ group and an hydroxyl group -OH. The

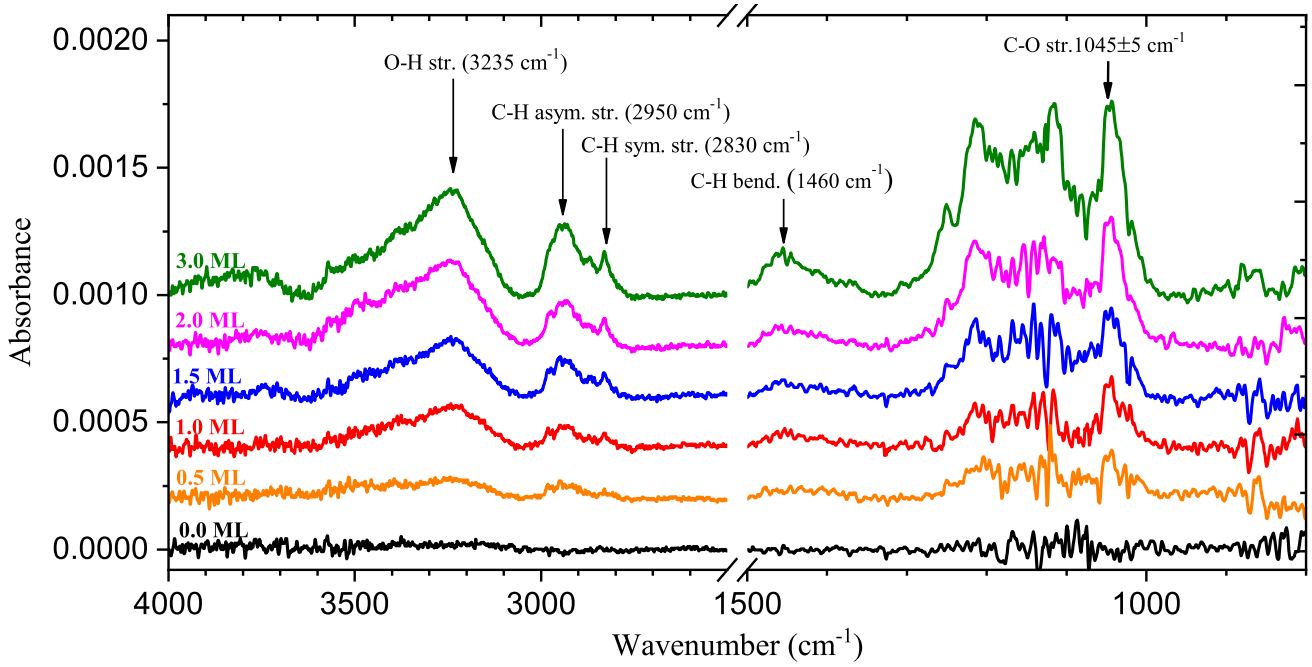


**Figure 5.** RAIRS spectra that show the growth of methanol IR bands with thickness up to 3 ML at a normalized flux $\Phi$=700 cps and $T_s$=10 K. All spectra were baseline corrected.

binding properties of the two groups are different, and when approaching the surface the accommodating properties of methanol may be different according to which of these different groups faces the substrate. However, this does not explain why there is a dependence with the surface temperature. The surface energy transfer (phonons) is supposed to vary with the temperature, but again phonons are very dependent on the type of the surface, and therefore the difference between the surfaces should be more pronounced if it were mostly induced by energy transfer. Nonetheless, on that point we can see that the CO film has the highest sticking coefficient, and the gold has the lowest one. This confirms that the rigidity of the surface, or its mass match, is an important point, and it probably explains why $^{13}CO$ (m/z=29), having the best mass match with $CH_3OH$ (m/z=32), turns out to have the highest sticking coefficient.

The common point for the three experiments is the building of the methanol film itself. From the TPD profiles of Fig. 3, we can see that there is only one desorption peak, which means that there is no specific binding site for methanol in a sub-monlayer regime on the surface, as can be seen for example for lighter molecules on crystalline surfaces (Ulbricht et al. 2002). This means that the major contribution of binding energy is the molecular film itself, in other words, methanol prefers to cluster or make islands rather than making a structure depending on the interaction with the substrate. Considering the asymmetry of methanol, it is clear that the positioning of one molecule with respect to another (or a set of other molecules that constitute the growing film) significantly changes its binding energy. In addition, to minimize its energy, a cluster of a few molecules must rearrange itself. This rearrangement cannot be done without a small excess of energy, that is an activation barrier. It is therefore possible that around 16 K, the methanol film no longer has enough degrees of freedom to reorganize itself in the short time that corresponds to the approach of a methanol molecule from the gas phase, and therefore cannot propose to the new molecule a favourable adsorption site. For this reason, a molecule arriving in a configuration with only a low binding energy, would have a better chance of bouncing back, at equal dissipation of its incident kinetic energy. Another way to say is that at 16 K, the reconstruction of the methanol film is hindered and only low coordinated adsorption sites are available. When the temperature decreases below this critical point, these low coordinated adsorption sites are anyway sufficient to be maintained on the surface. So the possible mechanism that increases the sticking efficiency with $T_s$ is the restructuring of the methanol film, and it counterbalances the usual mechanism making lower temperatures more favorable to trapping due to the longer interaction time and faster energy dissipation.

Nevertheless, whatever our explanations may be, this variation in sticking with surface temperature remains a surprise, and deserves to be studied in more detail. Even more so, the relatively low surface effect adds to the mystery, but it also may indicate that its origin is in the structuring of the methanol film itself. The role of methanol asymmetry could also be investigated in other complex molecules, such as $CH_3C_3$ or $CH_3CN$. Molecular dynamics calculations, and perhaps even quantum calculations given the temperature ranges, could also provide valuable insight into our experimental measurements.

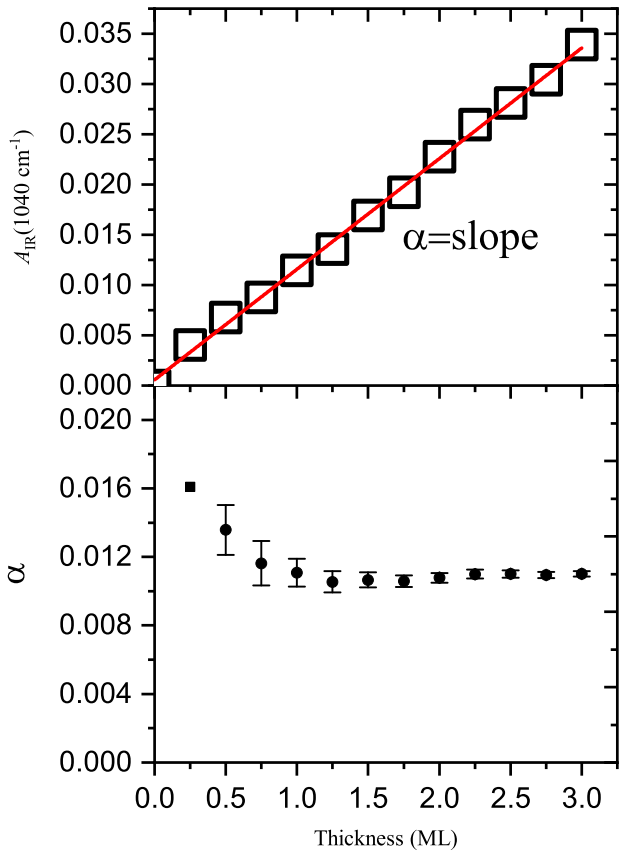


**Figure 6.** Top panel: integrated area of the 1045±5 cm$^{-1}$ band of methanol after deposition at the normalised flux Φ=700 cps at $T_s$=10 K versus film thickness. Bottom panel: $\alpha$-thickness dependence derived from IR spectra taken every two minutes on gold.

## 4 ASTROPHYSICAL IMPLICATIONS

In our experiments, we find that at $T_s$~ 16 K there is a decrease of the sticking coefficient by ~ 30% and an effective value of S($T_s$)=0.7 . Let's assume that this is due to an activation barrier. Under our experimental condition the gas is at room temperature (~ 293 K), and if the probability to overcome the barrier is $p = exp(-E_a/k_B T_g) = 0.7$, we find that the equivalent activation barrier is $E_a \simeq 124$ K/$k_B$. If we consider the physical conditions of a dark cloud having a gas and dust temperature of T=15 K, the sticking probability is $exp(-E_a/k_B T) \simeq 10^{-3}$. We can apply this to all our measurements, using the CO-substrate values as a reference. The choice of CO instead of $H_2O$ is motivated by the astrophysical context of accretion at later times. Anyhow, since the sticking coefficients of the different substrates are close, it would not change the main conclusion. These results are presented in Fig 10. The sticking is close to unity at very low temperatures and at the highest temperature ($T_s$>30 K). We can see that the sticking efficiency drops by two orders of magnitude under conditions between 10 K and 20 K, which are typical temperatures of molecular clouds. Moreover, the minimum in the sticking efficiency is shifted to lower temperatures, especially when the calculations are done using RAIRS data. This is due to the exponential reduction of the probability to stick with temperature, since the kinetic energy may be an efficient way to overcome the activation barrier.

Reasoning in terms of activation barrier is probably an oversimplification. Indeed, this activation barrier varies with surface temperature. Nevertheless, this approach shows the potential impact of this variation in sticking, if directly transposed to the conditions of the interstellar medium. A reduction of 2-3 orders of magnitude in the sticking of methanol would extend accretion times by as much, and thus make it possible to understand why this molecule can be observed in dark and cold environments, even if non-thermal desorption mechanisms were not efficient. Simply, methanol freeze-out may possibly be hindered.

Experimentally, it is very difficult to produce a cold beam of methanol, as it would condense on the cold parts of the apparatus well before entering the main chamber. Alternatively, it may be possible to play with the angle of deposition to reduce the perpendicular component of the kinetic energy, but unfortunately our set-up does not allow us to change the angle of deposition and adopt this technique. Therefore, the solution of the problem may come from the theory and/or the simulations. Molecular dynamic is possibly a good tool to explore this matter.

Molecular dynamics calculations (Bahr et al. 2008; Kong et al. 2019) show that the adsorption of a methanol on a layer of water occurs preferentially via the OH bond, leaving the methyl group facing upwards. But it appears that although the methanol-methanol interaction is weaker than with a water film, it remains important, of the order of 25 kJ/mol per H bond. In a methanol film, molecules tend to make several H bonds, and on graphite, methanol molecules are able to make clusters even at a very low coverage rate ($10^{-6}$ ML) at temperatures of about 180 K. These informations may then allow us to understand why the different surfaces do not seem to play a significantly different role. It is likely that the formation of a methanol cluster, or at least the interaction of one methanol with another methanol, and the formation of H bounds, plays a very important role in the formation of the film or surface clusters. It is questionable whether the presence of upwardly facing methyl groups does not prevent other molecules from sticking, or whether it is the difficulty of orienting and making the right H bonds that limits the capture rate around 15 K. As quoted by our anonymous referee, "assuming that the strongest potential interaction with a methanol molecule and the methanol ice surface would a single hydrogen bond interaction, the absence of any dangling OH on the methanol surface would mean that scattering from the surface might be more likely than adsorption unless partial accommodation of the incoming molecule on the surface provides sufficient energy to reorientate surface methanol species to expose OH groups". This point has to be compared with accurate calculations to see if it corresponds to the order of magnitude of the barrier we have derived here.

Until now, we do not yet understand the underlying reasons of the sticking variation as a function of surface temperature, and those of a minor impact of the substrate type. That is why it would not be wise to draw definitive conclusions on its astrophysical implications. With this paper, we simply wish to demonstrate that a more careful look, using both an experimental and a theoretical approach, has to be

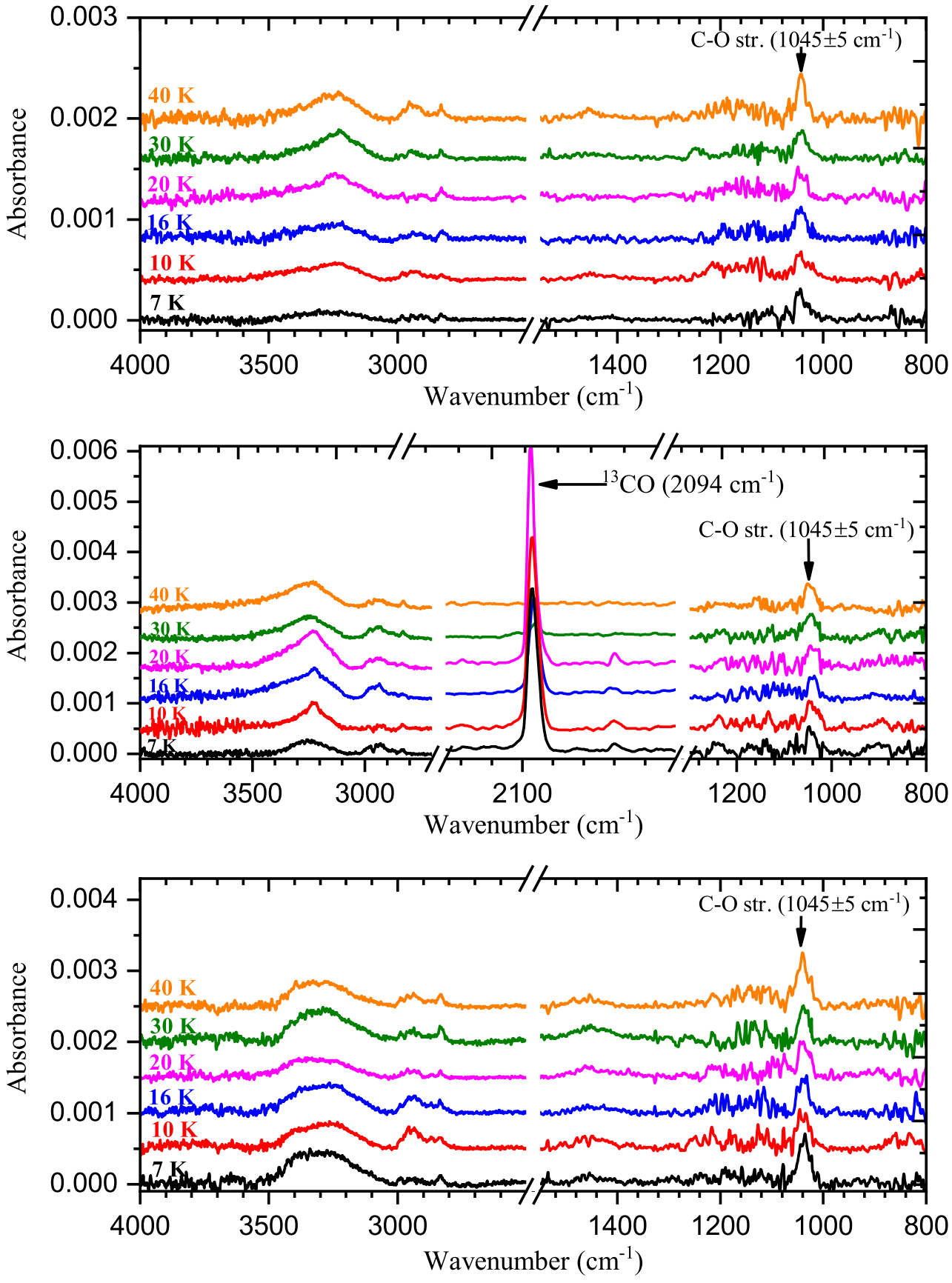


**Figure 7.** RAIRS spectra of 1 ML of methanol deposited at the normalized flux Φ=700 cps at various surface temperatures ($T_s$) on the substrate of gold (top panel), of $^{13}CO$ ice (middle panel), and of ASW ice (bottom panel).

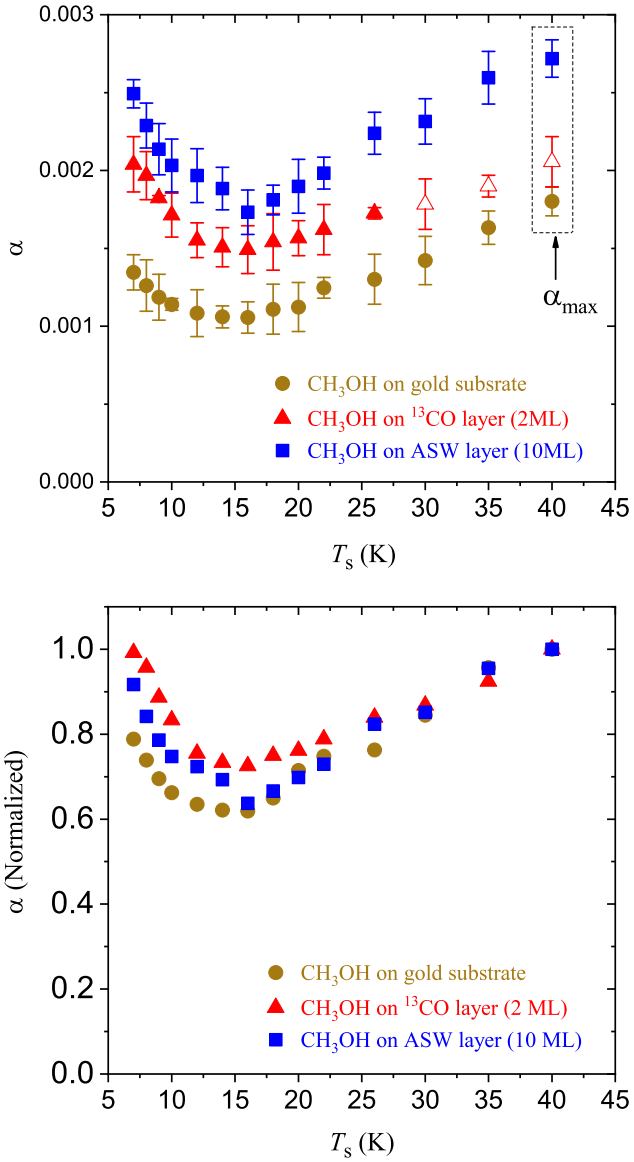


**Figure 8.** $\alpha$-profiles of methanol versus $T_s$ on surfaces (gold, $^{13}CO$, and ASW) at the normalized beam flux at $\Phi$=700 cps (top panel). $\alpha$-profiles normalized with respect to the value of $\alpha_{max}$ at $T_s$= 40 K (bottom panel).

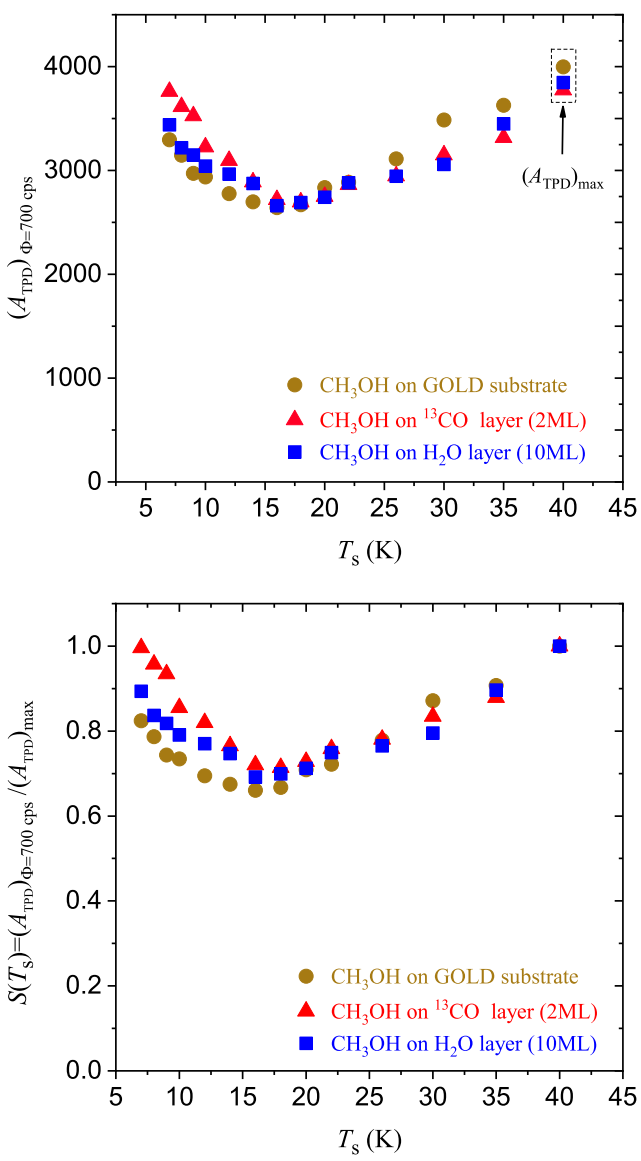


**Figure 9.** Integrated TPD peak area of methanol corresponding to depositions at the normalized beam flux ($\Phi$=700 cps) versus $T_s$ on surfaces of gold, $^{13}CO$, and ASW ice(top panel). Calculated sticking coefficients $S(T_s)$ versus the surface temperature (bottom panel).

taken at the problem of sticking of COMs at low temperatures.

## 5 CONCLUSIONS

Our experimental study of methanol sticking as a function of surface temperature (7 - 40 K) shows its variation with surface temperature. On three different cold surfaces (gold, $^{13}CO$, and ASW ice), a similar variation in methanol sticking can be observed. This variation has two antagonistic tendencies: the sticking of methanol 1) decreases rapidly with increasing the surface temperature from 7 to about 16 K, 2) increases slowly from 16 K to 40 K where it returns to a value similar to that found at 7 K. Depending on the type of the surface, a slight difference in the degree of sticking is observed at low temperatures. The gold surface has the lowest sticking efficiency while the $^{13}CO$ surface has the largest one, in agreement with mass matching arguments. The results obtained from TPD and RAIRS are consistent similar in their trend profiles as a function of surface temperature on different cold surfaces. In fact, the reduction in methanol sticking over a surface temperature of 16 K has been proven but raises questions about its origin. This may be due to the structuring properties of the methanol film, because of the asymmetry of this molecule. If our results obtained for a impinging gas at room temperature are abruptly extrapolated under dark cloud conditions, we find that the sticking would be reduced by two orders of magnitude. However, before ap-

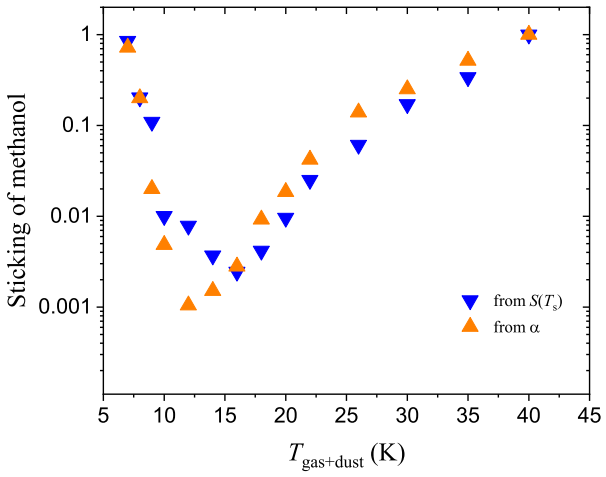


**Figure 10.** Calculated sticking coefficient assuming an activation barrier measured at $T_{gas}$ = 293 K, and in astrophysical conditions where $T_{gas}$ =$T_{dust}$ = 15 K. In blue are represented the values extracted from QMS data, S($T_s$), and in orange the values derived from RAIRS spectra, $\alpha$($T_s$).

plying this conversion law in space, it would be wiser to understand the physical origin of the variation in methanol sticking at low temperatures.

## ACKNOWLEDGEMENTS

This work was financially supported by the Egyptian government through the co-financed fellowship granted by the Science & Technology Development Fund (STDF; Project ID: 30565) and the Institut Français d' Égypte au Caire (IFE). So, authors acknowledge both STDF and IFE for supporting this research. KG thanks the Institute of Advance Studies of the university of Cergy Pontoise for its support. This work was supported by the Programme National "Physique et Chimie du Milieu Interstellaire (PCMI)" of CNRS/INSU with INC/INP co-funded by CEA and CNES and the DIM ACAV a funding programme of the Region Ile de France. $CH_3OH$ is a target molecule of SOLIS, a NOEMA key program led by P. Caselli & C. Ceccarelli, and this work is related to its scientific purposes.

## REFERENCES

Abou Mrad N., Duvernay F., Chiavassa T., Danger G., 2016, MNRAS, 458, 1234
Acharyya K., Fuchs G. W., Fraser H. J., van Dishoeck E. F., Linnartz H., 2007, A&A, 466, 1005
Bacmann A., Taquet V., Faure A., Kahane C., Ceccarelli C., 2012, A&A, 541, L12
Bahr S., Toubin C., Kempter V., 2008, J. Chem. Phys., 128, 134712
Bergin E. A., Tafalla M., 2007, ARA&A, 45, 339
Bertin M., et al., 2016, ApJ, 817, L12
Bisschop S. E., Fraser H. J., Öberg K. I., van Dishoeck E. F., Schlemmer S., 2006, A&A, 449, 1297
Bisschop S. E., Jørgensen J. K., van Dishoeck E. F., de Wachter E. B. M., 2007, A&A, 465, 913
Bockelee-Morvan D., Colom P., Crovisier J., Despois D., Paubert G., 1991, Nature, 350, 318
Bottinelli S., et al., 2010, ApJ, 718, 1100
Caselli P., Ceccarelli C., 2012, A&ARv, 20, 56
Ceccarelli C., et al., 2017, ApJ, 850, 176
Chaabouni H., Bergeron H., Baouche S., Dulieu F., Matar E., Congiu E., Gavilan L., Lemaire J. L., 2012, A&A, 538, A128
Charnley S. B., Tielens A. G. G. M., Kress M. E., 1995, MNRAS, 274, L53
Collings M. P., Anderson M. A., Chen R., Dever J. W., Viti S., Williams D. A., McCoustra M. R. S., 2004, MNRAS, 354, 1133
Congiu E., Sow A., Nguyen T., Baouche S., Dulieu F., 2020, Review of Scientific Instruments, 91, 124504
Cruz-Diaz G. A., Martín-Doménech R., Muñoz Caro G. M., Chen Y. J., 2016, A&A, 592, A68
Dartois E., Chabot M., Id Barkach T., Rothard H., Augé B., Agnihotri A. N., Domaracka A., Boduch P., 2019, A&A, 627, A55
Diekhöner L., Butler D., Baurichter A., Luntz A., 1998, Surface Science, 409, 384
Doronin M., Bertin M., Michaut X., Philippe L., Fillion J.-H., 2015, J. Chem. Phys., 143, 084703
Dulieu F., Congiu E., Noble J., Baouche S., Chaabouni H., Moudens A., Minissale M., Cazaux S., 2013, Scientific Reports, 3, 1338
Friberg P., Madden S. C., Hjalmarson A., Irvine W. M., 1988, A&A, 195, 281
Fulvio D., Sivaraman B., Baratta G. A., Palumbo M. E., Mason N. J., 2009, Spectrochimica Acta Part A: Molecular Spectroscopy, 72, 1007
Gadallah K. A. K., Marchione D., Koehler S. P. K., McCoustra M. R. S., 2017, Phys. Chem. Chem. Phys., 19, 3349
Galametz M., et al., 2016, MNRAS: Letters, 462, L36
Green S. D., Bolina A. S., Chen R., Collings M. P., Brown W. A., McCoustra M. R. S., 2009, MNRAS, 398, 357
Herbst E., van Dishoeck E. F., 2009, ARA&A, 47, 427
Jiménez-Serra I., et al., 2016, ApJ, 830, L6
Jiménez-Serra I., Viti S., Quénard D., Holdship J., 2018, ApJ, 862, 128
Kimmel G. A., Stevenson K. P., Dohnálek Z., Smith R. S., Kay B. D., 2001, J. Chem. Phys., 114, 5284
Kong X., Thomson E. S., MarkoviÄĞ N., Pettersson J. B. C., 2019, ChemPhysChem, 20, 2171
Kristensen L. E., van Dishoeck E. F., van Kempen T. A., Cuppen H. M., Brinch C., Jørgensen J. K., Hogerheijde M. R., 2010, A&A, 516, A57
Luna R., Molpeceres G., Ortigoso J., Satorre M. A., Domingo M., Maté B., 2018, A&A, 617, A116
Marchione D., McCoustra M. R. S., 2017, ACS Earth and Space Chemistry, 1, 310
Matar E., Bergeron H., Dulieu F., Chaabouni H., Accolla M., Lemaire J. L., 2010, J. Chem. Phys., 133, 104507
Minissale M., Moudens A., Baouche S., Chaabouni H., Dulieu F., 2016a, MNRAS, 458, 2953
Minissale M., Congiu E., Dulieu F., 2016b, A&A, 585, A146
Nguyen T., Baouche S., Congiu E., Diana S., Pagani L., Dulieu F., 2018, A&A, 619, A111
Noble J. A., Congiu E., Dulieu F., Fraser H. J., 2012, MNRAS, 421, 768
Öberg K. I., Fraser H. J., Boogert A. C. A., Bisschop S. E., Fuchs G. W., van Dishoeck E. F., Linnartz H., 2007, A&A, 462, 1187
Paardekooper D. M., Bossa J. B., Linnartz H., 2016, A&A, 592, A67
Palumbo M. E., 2006, A&A, 453, 903
Palumbo M., Baratta G., Leto G., Strazzulla G., 2010, J. Mol. Struct., 972, 64
Penteado E. M., Boogert A. C. A., Pontoppidan K. M., Ioppolo

S., Blake G. A., Cuppen H. M., 2015, MNRAS, 454, 531
Punanova A., et al., 2018, ApJ, 855, 112
Sandford S. A., Allamandola L. J., 1993, ApJ, 417, 815
Smith R. S., Matthiesen J., Kay B. D., 2014, J. Phys. Chem. A, 118, 8242
Taquet V., López-Sepulcre A., Ceccarelli C., Neri R., Kahane C., Charnley S. B., 2015, ApJ, 804, 81
Ulbricht H., Moos G., Hertel T., 2002, Physical Review B, 66, 075404
Vasyunin A. I., Herbst E., 2013, ApJ, 762, 86
Vasyunin A. I., Caselli P., Dulieu F., Jiménez-Serra I., 2017, ApJ, 842, 33
Walsh C., et al., 2016, ApJ, 823, L10
Walsh C., Vissapragada S., McGee H., 2018, in Cunningham M., Millar T., Aikawa Y., eds, IAU Symposium Vol. 332, IAU Symposium. pp 395–402 (arXiv:1710.01219), doi:10.1017/S1743921317007037
Wolff A. J., Carlstedt C., Brown W. A., 2007, J. Phys. Chem. c, 111, 5990

This paper has been typeset from a TEX/LATEX file prepared by the author.